

Article

# Assessment of Canopy Chlorophyll Content Retrieval in Maize and Soybean: Implications of Hysteresis on the Development of Generic Algorithms

Yi Peng <sup>1</sup>, Anthony Nguy-Robertson <sup>2</sup>, Timothy Arkebauer <sup>3</sup> and Anatoly A. Gitelson <sup>2,4,\*</sup>

<sup>1</sup> School of Remote Sensing and Information Engineering, Wuhan University, Wuhan 430072, China; ypeng@whu.edu.cn

<sup>2</sup> School of Natural Resources, University of Nebraska-Lincoln, Lincoln, NE 68588, USA; anthony.robertson@huskers.unl.edu

<sup>3</sup> Department of Agronomy and Horticulture, University of Nebraska-Lincoln, Lincoln, NE 68588, USA; tja@unl.edu

<sup>4</sup> Israel Institute of Technology (Technion), Haifa 320000, Israel

\* Correspondence: agitelson2@unl.edu

Academic Editors: Jose Moreno, Clement Atzberger and Prasad S. Thenkabail

Received: 4 January 2017; Accepted: 22 February 2017; Published: 2 March 2017

**Abstract:** Canopy chlorophyll content (Chl) closely relates to plant photosynthetic capacity, nitrogen status and productivity. The goal of this study is to develop remote sensing techniques for accurate estimation of canopy Chl during the entire growing season without re-parameterization of algorithms for two contrasting crop species, maize and soybean. These two crops represent different biochemical mechanisms of photosynthesis, leaf structure and canopy architecture. The relationships between canopy Chl and reflectance, collected at close range and resampled to bands of the Multi Spectral Instrument (MSI) aboard Sentinel-2, were analyzed in samples taken across the entirety of the growing seasons in three irrigated and rainfed sites located in eastern Nebraska between 2001 and 2005. Crop phenology was a factor strongly influencing the reflectance of both maize and soybean. Substantial hysteresis of the reflectance vs. canopy Chl relationship existed between the vegetative and reproductive stages. The effect of the hysteresis on vegetation indices (VI), applied for canopy Chl estimation, depended on the bands used and their formulation. The hysteresis greatly affected the accuracy of canopy Chl estimation by widely-used VIs with near infrared (NIR) and red reflectance (e.g., normalized difference vegetation index (NDVI), enhanced vegetation index (EVI) and simple ratio (SR)). VIs that use red edge and NIR bands (e.g., red edge chlorophyll index ( $CI_{red\ edge}$ ), red edge NDVI and the MERIS terrestrial chlorophyll index (MTCI)) were minimally affected by crop phenology (i.e., they exhibited little hysteresis) and were able to accurately estimate canopy Chl in two crops without algorithm re-parameterization and, thus, were found to be the best candidates for generic algorithms to estimate crop Chl using the surface reflectance products of MSI Sentinel-2.

**Keywords:** canopy chlorophyll content; reflectance; vegetation index; crop phenology; Sentinel-2

## 1. Introduction

Since chlorophyll is the main driver of light absorption and conversion of the absorbed light to stored chemical energy, it is an essential (although not unique) factor governing plant photosynthetic potential (e.g., [1,2]). Foliar chlorophyll content (Chl) provides useful information on leaf photosynthetic capacity as defined by the maximum rate of carboxylation ( $V_{max}$ , e.g., [3–5]).  $V_{max}$  directly relates to the RuBisCO enzyme that acts as a catalyst for carbon fixation within the leaf chloroplast. The leaf RuBisCO content is highly correlated with the foliar nitrogen (N) content because of the large proportion of N in photosynthetic machinery [6]. In addition to RuBisCO, much of the

incorporated foliar N is in chlorophyll, and therefore, strong correlations also exist between foliar Chl and N content [7–10]. However, the slope of the relationship N vs. photosynthetic capacity in crop declined for high N content [11]. It was also found that the relationship between Chl and N content at the canopy level is much stronger than at the leaf level (e.g., [10]).

Canopy Chl is defined as the total chlorophyll content per unit ground area in a contiguous group of plants [12]. It is well suited for quantifying canopy level N content and gross primary production [7,10,13–17]. Baret et al. [7] noted that canopy Chl is a physically sound quantity since it represents the optical path in the canopy where absorption by chlorophyll governs the radiometric signal, which is remotely detectable. Foliar Chl is commonly estimated using radiative transfer models (RTM; e.g., [18,19]) and vegetation indices (VI; see [20] for review). Canopy Chl is estimated using various techniques such as neural networks built using RTM-simulated reflectance (e.g., [21]) and chlorophyll-related VIs applied to close range and satellite data (e.g., [12,22,23]).

There are several issues with remote canopy Chl estimation. One relates to algorithm calibration by ground measurements. Canopy Chl is usually calculated as the product of foliar Chl and leaf area index (LAI) [7,10,12,15,22]. There are uncertainties in the ground truth data due to (a) foliar Chl determination either obtained analytically or retrieved from leaf reflectance and (b) LAI collected either destructively [24] or retrieved from canopy transmittance [25]. Acquisition of ground data for calibration and validation is especially challenging due to variable leaf area and foliar Chl distribution inside a canopy during the growing season (e.g., [24]).

Another substantial source of uncertainty relates to seasonal changes in canopy structural and biochemical traits that can significantly modify the spectral response of plants. Leaf structure and canopy architecture greatly influence leaf and canopy optical properties (e.g., [26,27]). In different phenological stages of vegetation development, the relationships between crop biophysical parameters and VIs are often significantly different (e.g., [28–30]). For example, the use of a single LAI vs. the normalized difference vegetation index (NDVI) relationship across the growing season led to substantial LAI overestimation in the vegetative stage and underestimation in the reproductive stage [31]. In deciduous broadleaf forests the enhanced vegetation index (EVI) vs. LAI relationships differed greatly in two distinct phenological stages [32]. The simple ratio (SR) index significantly decreased when senescent components began appearing in the canopy [33].

Regardless of the origin of the retrieval methods, statistical or physical analyses, the majority of the approaches retrieve biophysical properties of green vegetation only [34]. As a result, the models ignore the optical characteristics of senescent vegetation or the algorithm tends to perform poorly in the reproductive stage because it is not calibrated for senescent vegetation (e.g., [35–37]). A manipulative experiment and simulation analyses by RTM showed that senescent leaves significantly influence the spectral response of vegetation [38]. These results agree with [33,39,40], indicating that the presence of any significant fraction of dead material changes VI values.

Seasonal changes in the pigment pool and structural canopy properties greatly influence the light climate inside the canopy and modulate the extinction coefficient (e.g., [41]). For realistic modeling of reflectance, RTM should be fed by known vertical LAI and pigment content distributions, as well as their changes during the season. Despite theoretical and empirical evidence of the influence of senescing leaves on canopy spectral responses, documented changes in canopy structural properties during the season and uncertainties in canopy Chl and other biophysical property estimation, these issues have not been adequately elaborated upon and addressed. It is important for monitoring crops with different structural properties when the spatial resolution of the sensor is low (e.g., comparable to field size or larger) and in regions with mixed-use cropping practices (e.g., maize/soybean rotation) requiring generic algorithms that do not need re-parameterization for different crops.

The goal of this study is to develop remote sensing techniques to accurately estimate canopy Chl during the entire growing season in two contrasting crop species, maize and soybean, representing different biochemical mechanisms of photosynthesis (C3 and C4), leaf structures (monocot and dicot) and canopy architectures (spherical in maize; heliotropic in soybean) without re-parameterization of algorithms for each crop. The first objective was to identify spectral bands sensitive to canopy Chl and to gain insights into the effect of crop phenology on reflectance in these spectral bands (i.e., to quantify the hysteresis of the reflectance vs. canopy Chl relationship). The second objective was to analyze the effect of the hysteresis on VIs used for canopy Chl estimation and explore VIs that are minimally affected by crop phenology. The final objective was to explore generic algorithms for canopy Chl estimation by VIs simulated from reflectance in the spectral bands of the Multi Spectral Instrument (MSI) sensor on board the Sentinel-2 satellite with spectral and spatial resolution found to be suitable for estimating crop biophysical characteristics [17,34,42,43].

## 2. Materials and Methods

### 2.1. Study Area

The study consists of three AmeriFlux sites (US-Ne1, US-Ne2 and US-Ne3), located at the University of Nebraska-Lincoln Agricultural Research and Development Center near Mead, Nebraska, USA, <http://public.ornl.gov/ameriflux/site-select.cfm>. The sites are about 60 ha each and within 5 km of each other. Site 1 was planted in continuous maize and was equipped with a center-pivot irrigation system. Sites 2 and 3 were both planted in a maize-soybean rotation, with maize planted in odd years and soybean planted in even years. Site 2 was irrigated in the same way as Site 1, while Site 3 relied entirely on rainfall for moisture. More details about these sites are in [44]. The field campaigns were carried out biweekly during the growing seasons (from May to September) from 2001 to 2005 to collect crop parameters and canopy spectra.

### 2.2. Canopy Reflectance

Hyperspectral radiometers were mounted on an all-terrain sensor platform for canopy reflectance measurements [45,46]. A dual-fiber optic system with two inter-calibrated Ocean Optics USB2000 radiometers was used to collect radiometric data in the range 400 to 1100 nm with a spectral resolution of about 1.5 nm. One radiometer was equipped with a 25° field-of-view optical fiber pointing downward to measure the upwelling radiance of the canopy. The position of this radiometer was kept at nadir approximately 5.4 m above the canopy throughout the growing season, yielding a sampling area with a diameter of around 2.4 m at the top of the canopy. The second radiometer was equipped with an optical fiber and a cosine diffuser pointing upward to measure downwelling irradiance. Percent canopy reflectance was then calculated from the ratio of upwelling radiance to the simultaneously-measured downwelling irradiance.

Radiometric data were collected close to solar noon (between 11:00 and 13:00 local time), when changes in solar zenith angle were minimal. For each study site, six randomly selected plots were established, and each plot was measured with six randomly selected sampling points (details in [47]). Thus, 36 reflectance measurements were obtained per site, and their median was used as the site canopy reflectance.

### 2.3. Destructive Measurements of Leaf Area Index

Green LAI was determined destructively in the lab from samples collected in six small plots (20 m × 20 m) established within each site. These plots represented all major soil and crop production zones within each site [44]. Plants from a 1-m length of either of two rows within each plot were collected and the total number of plants recorded. Plants were kept on ice and transported to the lab where they were separated into green leaves, dead leaves and litter components. All green leaves were run through an area meter (Model LI-3100, Li-Cor, Inc., Lincoln, Nebraska), and the leaf area per plant

was measured. For each plot, the green leaf area per plant was multiplied by the plant population to obtain a green LAI. Green LAI for the six plots was then averaged as a site-level value (see [42] for more details).

#### 2.4. Chlorophyll Content Measurements at the Leaf and Canopy Level

During growing seasons from 2001 through 2005, spectral reflectance measurements of the ear leaf in maize and the top-most fully expanded leaf in soybean were collected biweekly in three sites using an Ocean Optics radiometer. Maize and soybean leaves were transported to the lab, and leaf Chl content ( $\text{Chl}_{\text{leaf}}$ ) was determined analytically (details in [12,42]). A linear relationship of  $\text{Chl}_{\text{leaf}}$  vs. red edge chlorophyll index ( $\text{CI}_{\text{red edge}}$ ) was then calibrated with a determination coefficient  $R^2 = 0.95$  [12]:

$$\text{Chl}_{\text{leaf}} (\text{mg} \cdot \text{Chl} \cdot \text{m}^{-2}) = 37.904 + 1353.7 \times \text{CI}_{\text{red edge}} \quad (1)$$

$\text{CI}_{\text{red edge}} = (\rho_{\text{NIR}} / \rho_{\text{red edge}}) - 1$ , where  $\rho_{\text{NIR}}$  is the average reflectance in the near infrared (NIR) range from 770 through 800 nm and  $\rho_{\text{red edge}}$  is the average reflectance in the range from 720 to 730 nm [48]. The reproductive stage was defined as the period between maximal canopy Chl and the end of the season. In maize, this corresponds to the usual way of separating the vegetative from the reproductive stage, but in soybean, it means that our definition of the vegetative stage also includes the first few reproductive sub-stages (up until R4, most likely), which is just prior to seed filling [49].

#### 2.5. Vegetation Indices

The third objective of this study is to find VIs applicable to the 20-m resolution MSI aboard the Sentinel-2 polar-orbiting satellite, which is showing great potential for land surface parameter estimations [50–52]. The collected field reflectance spectra were resampled to represent the spectral bands of MSI [43] by calculating the average reflectance over the bandwidth of the respective MSI bands. This approximation was applied since the spectral response functions of the MSI spectral bands are close to rectangular [43,53]. Using the simulated MSI reflectance, VIs (Table 1) were calculated and compared with the corresponding canopy Chl. The total sample size for this study was 191 for maize and 73 for soybean.

**Table 1.** Vegetation indices (VI) tested in this study.  $R_{\text{blue}}$ ,  $R_{\text{green}}$ ,  $R_{\text{red}}$ ,  $R_{705}$ ,  $R_{740}$  and  $R_{\text{NIR}}$  refer to reflectance simulated in Multi Spectral Instrument (MSI) spectral bands of 430 to 450 nm, 543 to 577 nm, 650 to 80 nm, 692 to 712 nm, 732 to 748 nm and 773 to 793 nm, respectively.

Vegetation Index	Formula	Reference
Simple ratio (SR)	$R_{\text{NIR}} / R_{\text{red}}$	Jordan, 1969 [54]
Normalized difference vegetation index (NDVI)	$(R_{\text{NIR}} - R_{\text{red}}) / (R_{\text{NIR}} + R_{\text{red}})$	Rouse et al., 1974 [55]
Enhanced vegetation index (EVI)	$2.5 (R_{\text{NIR}} - R_{\text{red}}) / (R_{\text{NIR}} + 6 R_{\text{red}} - 7.5 R_{\text{blue}} + 1)$	Huete et al., 1997 [56]
Green NDVI	$(R_{\text{NIR}} - R_{\text{green}}) / (R_{\text{NIR}} + R_{\text{green}})$	Vina and Gitelson, 2005 [57]
Green chlorophyll index ( $\text{CI}_{\text{green}}$ )	$(R_{\text{NIR}} / R_{\text{green}}) - 1$	Gitelson et al., 2003 [22]
Red edge NDVI <sub>705</sub>	$(R_{\text{NIR}} - R_{705}) / (R_{\text{NIR}} + R_{705})$	Vina and Gitelson, 2005 [57]
Red edge NDVI <sub>740</sub>	$(R_{\text{NIR}} - R_{740}) / (R_{\text{NIR}} + R_{740})$	Vina and Gitelson, 2005 [57]
MERIS terrestrial chlorophyll index (MTCI)	$(R_{\text{NIR}} - R_{705}) / (R_{705} - R_{660})$	Dash and Curran, 2004 [23]
Red edge chlorophyll index ( $\text{CI}_{705}$ )	$(R_{\text{NIR}} / R_{705}) - 1$	Gitelson et al., 2003 [22]
Red edge chlorophyll index ( $\text{CI}_{740}$ )	$(R_{\text{NIR}} / R_{740}) - 1$	Gitelson et al., 2003 [22]

#### 2.6. Development of Algorithms for Remote Estimation of Canopy Chl

The k-fold cross-validation procedure [58,59] was used to establish the algorithms for estimating canopy Chl using VIs. The original samples were randomly split into k mutually exclusive sets ( $k = 10$ ), and they were trained and tested k times. For each time,  $k - 1$  sets were used iteratively as training data for calibrating the coefficients ( $\text{Coef}_i$ ) of the relationship, and the remaining single set was retained as the validation dataset to obtain the determination coefficient ( $R^2_i$ ), RMSE<sub>i</sub> and normalized root mean square error (NRMSE)<sub>i</sub> for the established algorithm. This procedure was then repeated k times,

with each of the  $k$  sets used exactly once as the validation data. The results from  $k$  iterations then were averaged to produce a single estimation:

$$\begin{aligned} \text{Coef} &= \frac{1}{k} \sum_{i=1}^k (\text{Coef})_i \quad R^2 = \frac{1}{k} \sum_{i=1}^k (R^2)_i \\ \text{RMSE} &= \frac{1}{k} \sum_{i=1}^k (\text{RMSE})_i \quad \text{NRMSE} = \frac{1}{k} \sum_{i=1}^k (\text{NRMSE})_i \end{aligned} \quad (2)$$

This approach reduces the dependence on a single random partition into calibration and validation datasets. By repeating the training procedure  $k$  times, all observations were used for both calibration and validation, with each observation used for validation one time.

To assess the accuracy of estimating canopy Chl by different VIs, the noise equivalents (NE $\Delta$ Chl) of VIs were compared. The noise equivalent was calculated as:

$$\text{NE}\Delta \text{ Chl} = \text{RMSE (VI vs. canopy Chl)} / (d(\text{VI})/d(\text{canopy Chl})), \quad (3)$$

where  $d(\text{VI})/d(\text{canopy Chl})$  is the first derivative of the best fit function of the VI vs. canopy Chl relationship with respect to canopy Chl, and  $\text{RMSE}(\text{VI vs. canopy Chl})$  is the root mean square error of the best fit function of this relationship [57].

To determine if there was a statistically-significant difference between two relationships, the two-sample  $t$ -test approach [60] was used. This approach was run on samples for two tested relationships using the Data Analysis Tools in Excel 2010 (Microsoft Corp., Redmond, WA, USA). If the  $p$ -value obtained from the test was lower than 0.05, the observed difference between two relationships was convincing enough to be significant.

### 3. Results

#### 3.1. Canopy Reflectance vs. Canopy Chl Relationships

For the reflectance vs. canopy Chl relationships in the photosynthetically-active radiation (PAR) spectral region, there was a substantial and statistically-significant hysteresis between the two phenological stages in maize (Figure 1A–D; Table 2). In the PAR MSI spectral bands, maize reflectance decreased with an increase in canopy Chl for both the vegetative and reproductive stages. However, for low to moderate canopy Chl (below  $2 \text{ g}\cdot\text{m}^{-2}$ ), reflectance in the vegetative stage was consistently higher than in the reproductive stage (Figure 1A–D). In the green (around 560 nm) and shortwave red edge (around 705 nm) bands, the difference in reflectance between the two stages was somewhat smaller than in the blue and the red bands (Figure 1B,D). In the longwave red edge (around 740 nm) and NIR bands, reflectance increased with increases in canopy Chl, and the difference in reflectance between the two stages was statistically significant only for the longwave red edge band (Figure 1E,F; Table 2). However, the significance of this difference was weaker than that of the visible and shortwave red edge bands ( $p$ -value = 0.0015 for longwave red edge band vs.  $p$ -value  $< 10^{-6}$  for visible and shortwave red edge bands).

In soybean, the hysteresis in the blue and red bands was pronounced, and the relationships in the vegetative and reproductive stages were statistically different, i.e., the results were similar to maize (Figure 2A,C; Table 2). However, in the green, red edge and NIR bands, the relationships were not statistically different (Figure 2B,D–F; Table 2). For the reproductive stage in soybean, the red edge reflectance was slightly higher than in the vegetative stage (Figure 2D,E), which was in contrast to maize. The difference between the vegetative and reproductive stages in the NIR band was not statistically significant for either maize or soybean (Table 2).

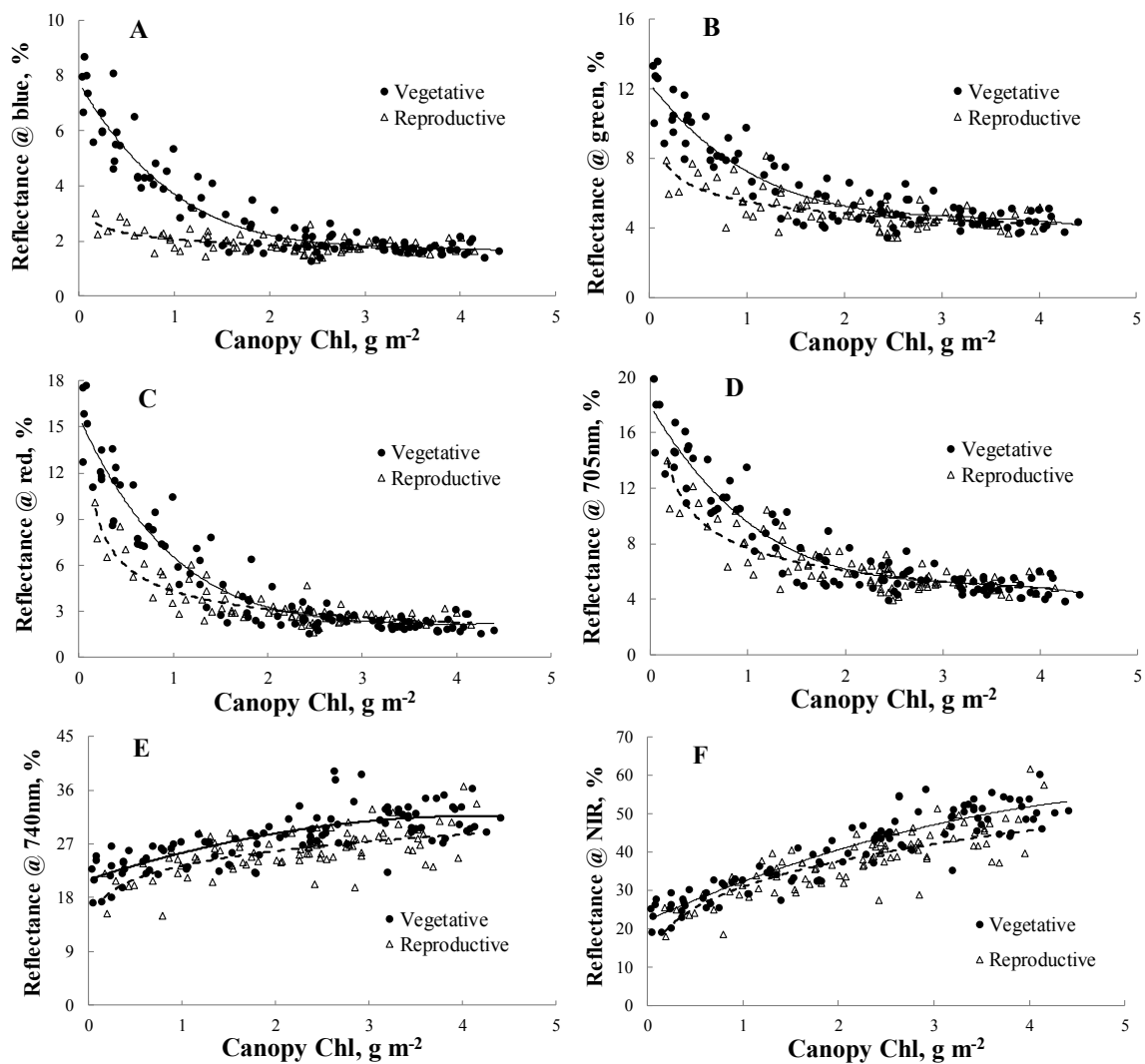


**Figure 1.** Relationships between reflectance simulated at MSI spectral bands and canopy Chl for maize in blue (A), green (B), red (C), shortwave red edge (705 nm) (D), longwave red edge (740 nm) (E) and NIR (F) bands.

**Table 2.** The results of statistical analysis of the difference in reflectance vs. canopy Chl relationships between vegetative and reproductive stages. Reflectance was simulated for the six MSI spectral bands. The  $p$ -value was retrieved from the two-sample  $t$ -test approach to indicate the difference of two relationships. If the  $p$ -value  $< 0.05$ , the observed difference between two relationships was convincing enough to be significant.

Band	Maize	$p$ -Value	Soybean	$p$ -Value
Blue	$R_{\text{rep}} < R_{\text{veg}}$	$1.58 \times 10^{-13}$	$R_{\text{rep}} < R_{\text{veg}}$	$1.12 \times 10^{-6}$
Green	$R_{\text{rep}} < R_{\text{veg}}$	$3.75 \times 10^{-11}$	$R_{\text{rep}} \approx R_{\text{veg}}$	0.04
Red	$R_{\text{rep}} < R_{\text{veg}}$	$9.36 \times 10^{-8}$	$R_{\text{rep}} < R_{\text{veg}}$	$4.02 \times 10^{-14}$
Shortwave red edge (705 nm)	$R_{\text{rep}} < R_{\text{veg}}$	$6.20 \times 10^{-7}$	$R_{\text{rep}} \approx R_{\text{veg}}$	0.35
Longwave red edge (740 nm)	$R_{\text{rep}} < R_{\text{veg}}$	$1.50 \times 10^{-3}$	$R_{\text{rep}} \approx R_{\text{veg}}$	0.06
NIR	$R_{\text{rep}} \approx R_{\text{veg}}$	0.55	$R_{\text{rep}} \approx R_{\text{veg}}$	0.15

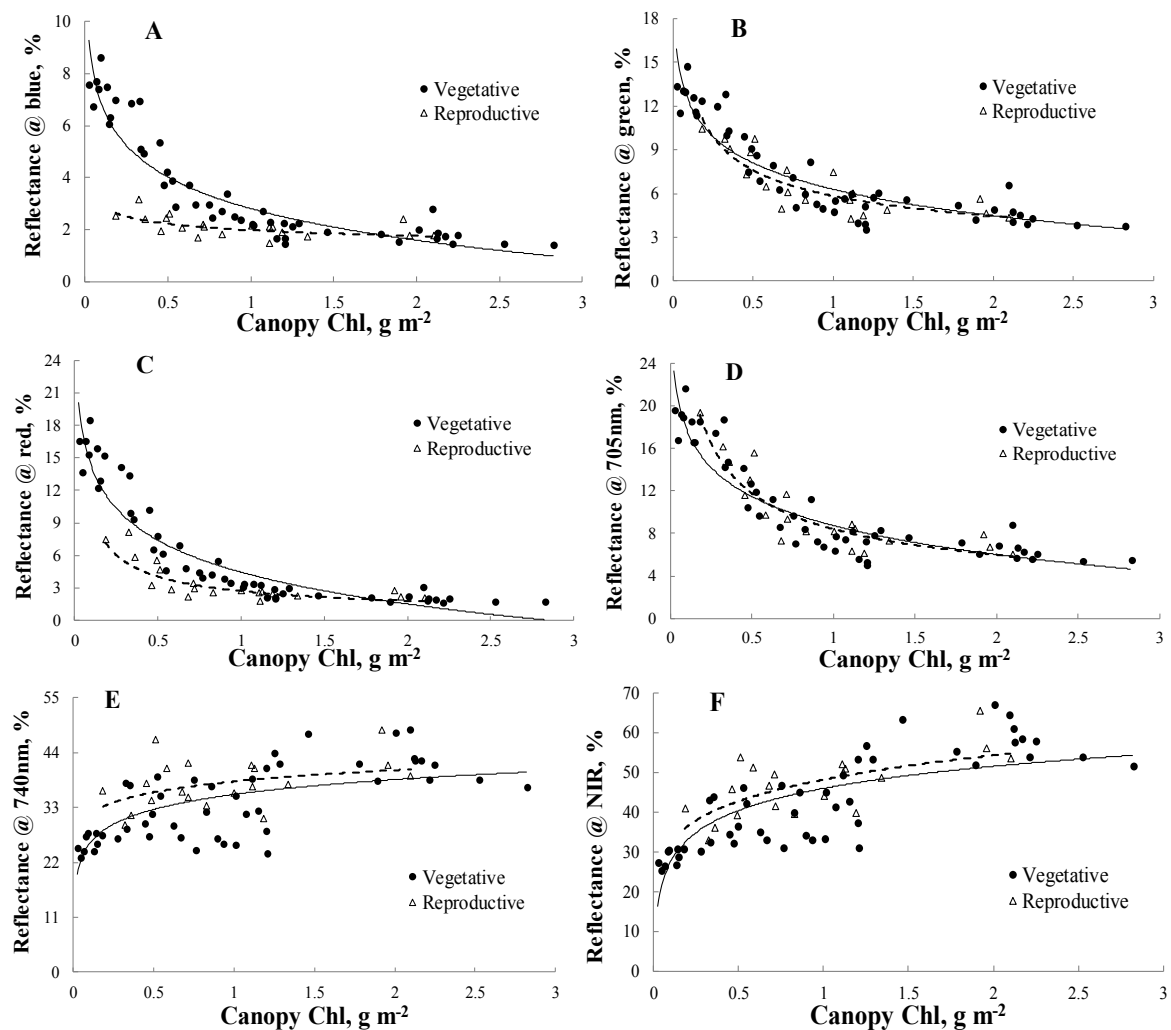


**Figure 2.** Relationships between reflectance simulated at MSI spectral bands and canopy Chl for soybean in blue (A), green (B), red (C), shortwave red edge (705 nm) (D), longwave red edge (740 nm) (E) and NIR (F) bands.

Other studies have demonstrated that as LAI increased, canopy Chl and NIR reflectance increased correspondingly [24,61]. While a strong relationship exists between canopy Chl and green LAI, this relationship exhibits hysteresis due to leaf Chl varying over a growing season. For the same green LAI, total canopy Chl in a reproductive stage may be much lower than that in a vegetative stage [16,61]. This is due to green LAI representing a subjective metric, as it depends on a visual inspection and interpretation of leaf color (e.g., [24]).

Reflectance spectra of maize and soybean with similar canopy Chl in the vegetative and reproductive stages, presented in Figure 3, illustrate how strongly and differently crop phenology affected the reflectance of these two species at low to moderate canopy Chl (i.e., canopy Chl < 1.5 g·m<sup>-2</sup>). In maize, reflectance was much lower for the reproductive stage than for the vegetative stage, especially in the blue and red bands. Soybean reflectance in the red and blue bands was slightly lower in the reproductive stage, but the difference was minimal in the green and red edge bands. For soybean, the NIR and longwave red edge bands reflectance was slightly higher in the reproductive stage. Note that for both maize and soybean, the difference in reflectance between the two stages was most pronounced in the blue and red bands, while the reflectance in the red edge bands was closer in the two stages compared to other spectral bands.

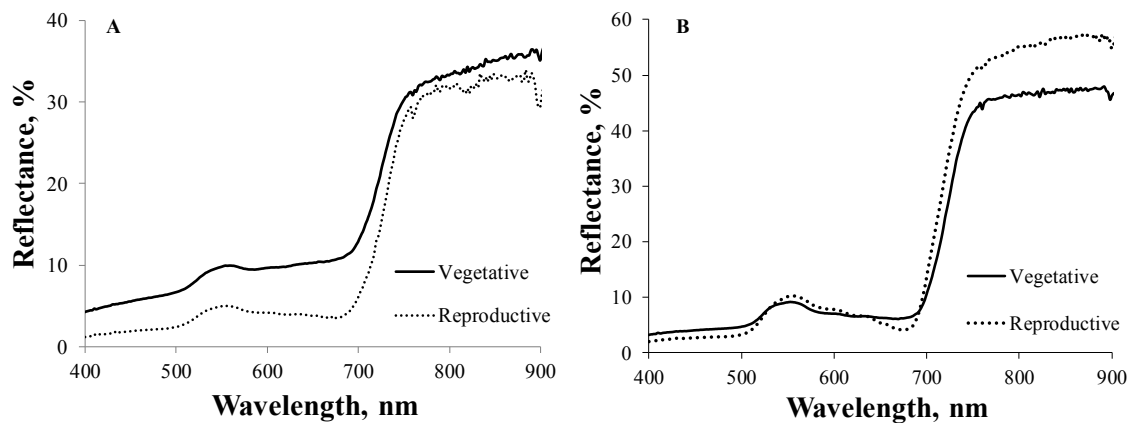


**Figure 3.** Reflectance spectra of crops with similar canopy Chl in the vegetative and reproductive stages. (A) Maize spectra collected in the vegetative stage (21 June, canopy Chl =  $0.98 \text{ g}\cdot\text{m}^{-2}$ ) and in the reproductive stage (6 September, canopy Chl =  $0.99 \text{ g}\cdot\text{m}^{-2}$ ). (B) Soybean spectra collected in the vegetative stage (8 July, canopy Chl =  $0.52 \text{ g}\cdot\text{m}^{-2}$ ) and in the reproductive stage (12 September, canopy Chl =  $0.51 \text{ g}\cdot\text{m}^{-2}$ ).

### 3.2. Vegetation Indices vs. Canopy Chl Relationships

The hysteresis of the reflectance vs. canopy Chl relationships affects the accuracy of canopy Chl estimation using vegetation indices. VI vs. canopy Chl relationships across entire growing seasons were established for maize and soybean, respectively (Figures 4 and A1). In both species, with the same canopy Chl, NDVI and SR were higher in the reproductive stage than in the vegetative stage, especially for canopy Chl  $< 1 \text{ g}\cdot\text{m}^{-2}$  (NDVI in Figure 4A,B and SR in Figure A1(A,B)). Soybean EVI was higher in the reproductive stage than in the vegetative stage, while maize EVI behaved similarly in both stages (Figure 4C,D). The hysteresis of  $\text{CI}_{\text{green}}$ , green NDVI,  $\text{CI}_{705}$  and red edge NDVI<sub>705</sub> was weaker, with the VIs slightly higher in the reproductive stage (Figure A1(C–J)). Unlike other indices, MTCI was lower in the reproductive stage than in the vegetative stage for both maize and soybean (Figure 4E,F). This is due to a more pronounced hysteresis of reflectance in the red region than in the red edge region (Figure 3); thus, the MTCI denominator ( $R_{\text{red edge}} - R_{\text{red}}$ ) was higher in the reproductive stage causing lower MTCI values. Minimal impacts from hysteresis were observed for the  $\text{CI}_{740}$  and red edge NDVI<sub>740</sub> in both species (Figure 4G,H, Figure A1(K,L)).

For each crop, algorithms for estimating canopy Chl for the entire growing season were devised using a 10-fold cross-validation procedure for VIs having linear or close to linear relationships with canopy Chl (Table 3). In both species, estimation errors were highest for VIs using NIR and red reflectance (e.g., EVI and SR). Hysteresis between the two growing stages affected canopy Chl estimates much less in VIs utilizing NIR and either green or red edge reflectance. In maize, MTCI,  $\text{CI}_{740}$  and red edge NDVI<sub>740</sub> were the most accurate with the lowest NRMSE values. In soybean,  $\text{CI}_{\text{green}}$  and  $\text{CI}_{705}$  had the best error metrics when estimating canopy Chl.

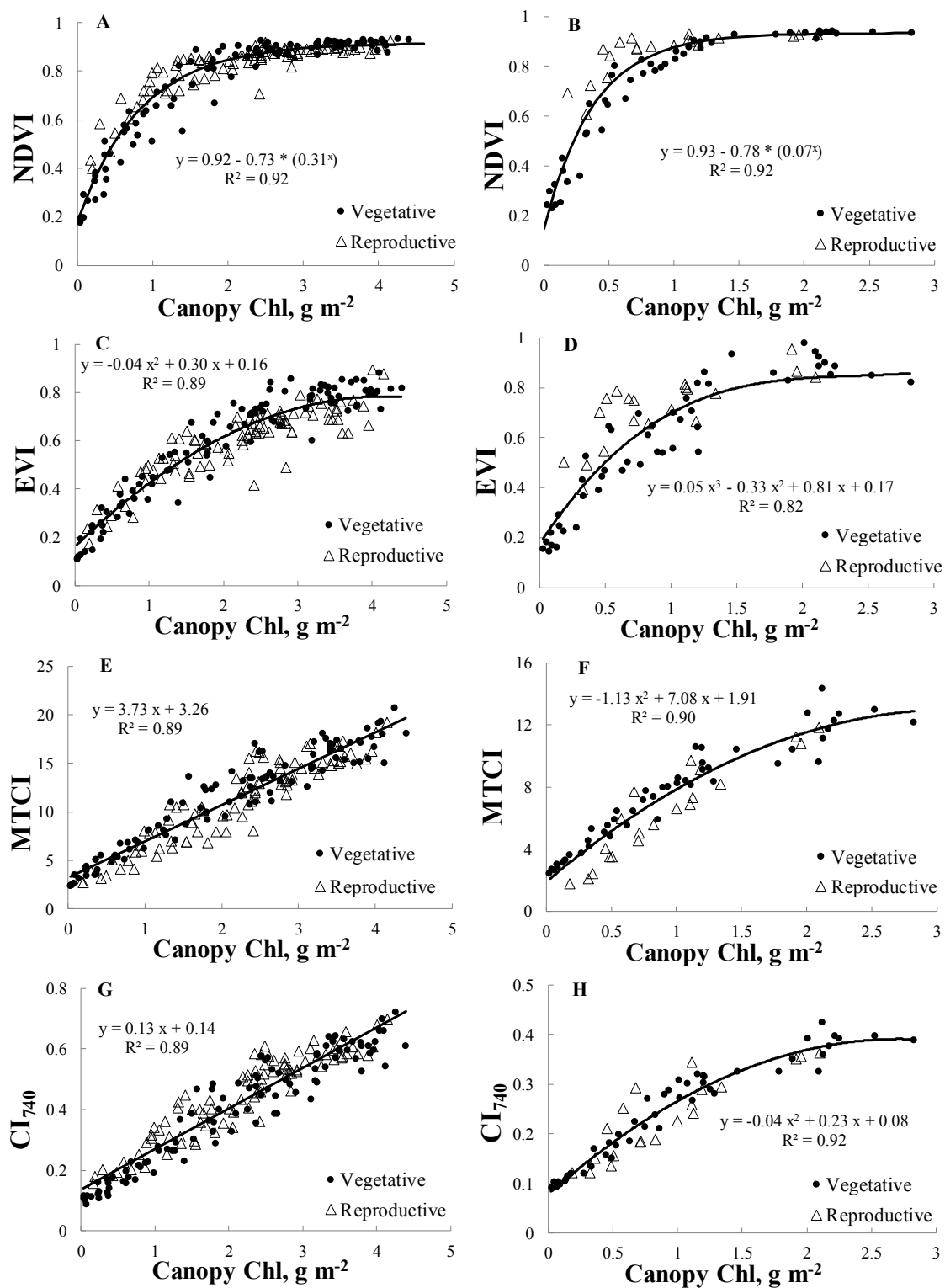


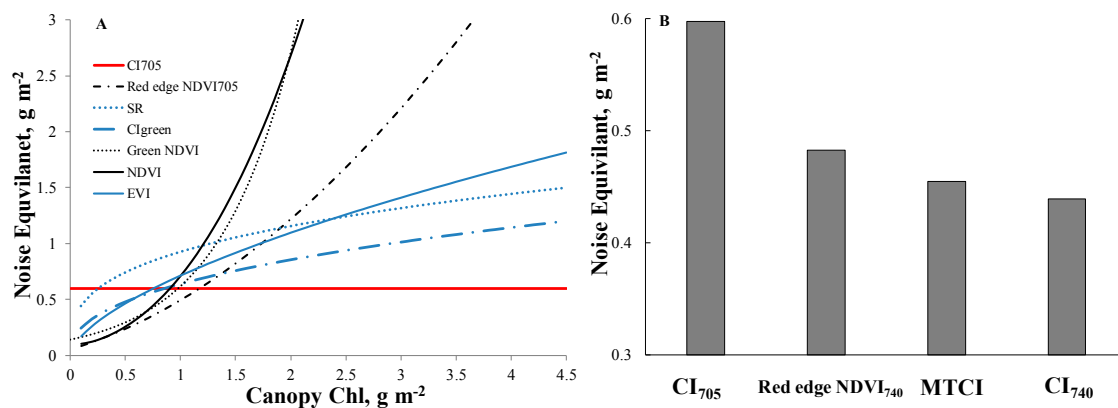
**Figure 4.** Relationships of VI vs. canopy Chl during both growth stages for NDVI in maize (A), NDVI in soybean (B), EVI in maize (C), EVI in soybean (D), MTCI in maize (E), MERIS terrestrial chlorophyll index (MTCI) in soybean (F),  $CI_{740}$  in maize (G) and  $CI_{740}$  in soybean (H). The solid line represents the best-fit-function of VI vs. canopy Chl developed using samples from the vegetative and reproductive stages combined.

**Table 3.** Algorithms, normalized root mean square error (NRMSE) in  $\text{g}\cdot\text{m}^{-2}$  and determination coefficient ( $R^2$ ) of canopy Chl estimation during the entire growing season in maize and soybean.

VI	Maize			Soybean		
	Algorithm	NRMSE	$R^2$	Algorithm	NRMSE	$R^2$
EVI	$y = 5.54x - 1.11$	0.112	0.89	$y = 2.51x - 0.59$	0.139	0.82
SR	$y = 0.14x + 0.30$	0.117	0.80	$y = 0.0653x + 0.0415$	0.093	0.87
$CI_{\text{green}}$	$y = 0.35x - 0.21$	0.103	0.85	$y = 0.182x - 0.168$	0.082	0.88
$CI_{705}$	$y = 0.36x + 0.15$	0.096	0.86	$y = 0.25x - 0.0778$	0.075	0.94
Red edge $NDVI_{740}$	$y = 18.8x - 1.06$	0.089	0.91	$y = 17.1x - 0.832$	0.093	0.92
MTCI	$y = 0.24x - 0.54$	0.087	0.89	$y = 0.202x - 0.473$	0.089	0.90
$CI_{740}$	$y = 6.68x - 0.67$	0.087	0.89	$y = 6.85x - 0.676$	0.089	0.92

### 3.3. Generic Algorithms for Canopy Chl Estimation in Maize and Soybean

Generic algorithms were developed using 10-fold cross-validation procedures to estimate canopy Chl in both crop species during the entire growing season. Noise equivalent values were calculated for these algorithms (Figure 5). Normalized difference VIs using NIR and either red, green or 705-nm reflectance ( $NDVI$ , green  $NDVI$  and red edge  $NDVI_{705}$ ) accurately estimated low canopy Chl values; however, the uncertainties for canopy Chl  $>1 \text{ g}\cdot\text{m}^{-2}$  increased almost exponentially (Figure 5A). The noise equivalents of VIs using NIR and either green or red bands ( $CI_{\text{green}}$ , SR and EVI) were two-fold higher than those using red edge and NIR bands (red edge  $NDVI_{740}$ ,  $CI_{740}$ , MTCI and  $CI_{705}$ ). Very close linear relationships were found for red edge  $NDVI_{740}$ ,  $CI_{740}$ , MTCI (Figure 5B) and  $CI_{705}$  (Figure 5A,B). Note that  $CI_{705}$  was less accurate in estimating canopy Chl than  $CI_{740}$  (Figure 5B).  $CI_{740}$ , red edge  $NDVI_{740}$  and MTCI outperformed other VIs tested with noise equivalent values below  $0.5 \text{ g}\cdot\text{m}^{-2}$  for the whole range of canopy Chl variation (Figure 5B).

**Figure 5.** Noise equivalent of canopy Chl estimating in maize and soybean combined by VIs calculated using reflectance simulated at MSI spectral bands for (A)  $NDVI$ , green  $NDVI$ , red edge  $NDVI_{705}$ , SR, EVI,  $CI_{\text{green}}$  and  $CI_{705}$  and (B)  $CI_{705}$ , MTCI, red edge  $NDVI_{740}$  and  $CI_{740}$ . Note that the maximum noise equivalent (y-axis value) in (A) is five-fold higher than in (B).

$CI_{740}$ , red edge  $NDVI_{740}$  and MTCI were used in established generic algorithms for canopy Chl estimation in maize and soybean combined (Figure 6, Table 4). All of these VIs were able to accurately estimate canopy Chl for the two crops combined with  $R^2$  above 0.9 and RMSE below  $0.38 \text{ g}\cdot\text{m}^{-2}$ .

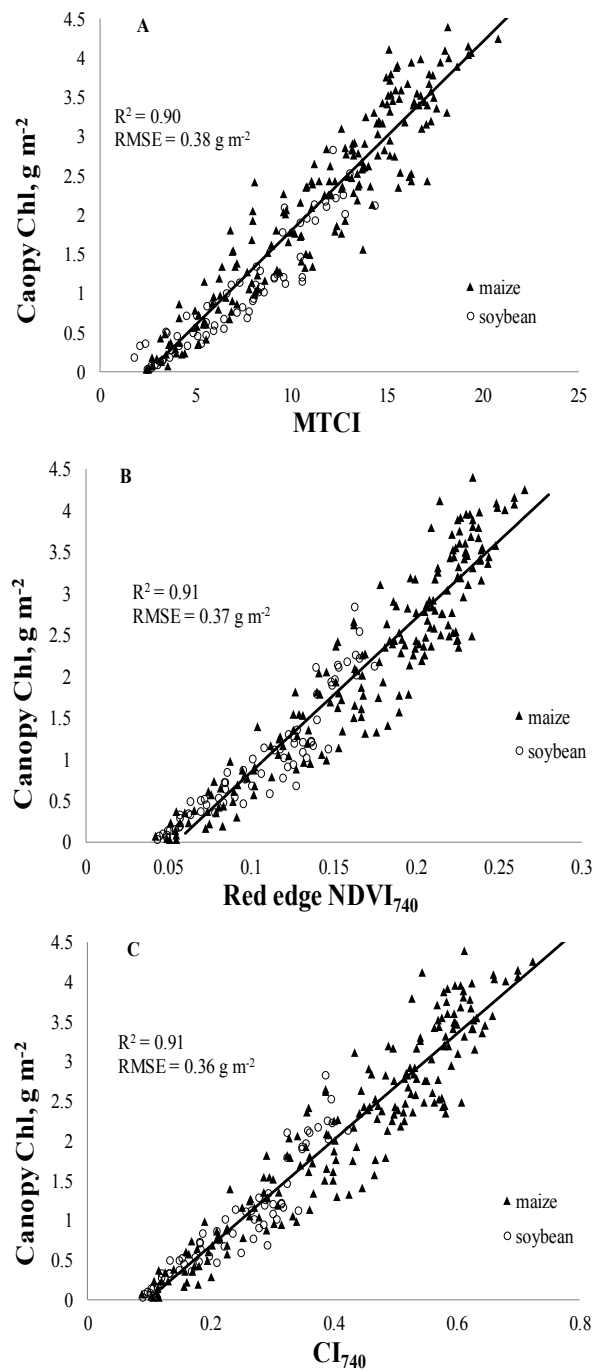


**Figure 6.** Relationships between VIs calculated using reflectance simulated in MSI spectral bands and canopy Chl in maize and soybean combined for MTCI (A), red edge NDVI<sub>740</sub> (B) and CI<sub>740</sub> (C).

**Table 4.** Algorithms, determination coefficients ( $R^2$ ) and root mean square error (RMSE) of canopy Chl estimated using three different vegetation indices in maize and soybean combined.

Canopy Chl in $\text{g}\cdot\text{m}^{-2}$	$R^2$	RMSE, $\text{g}\cdot\text{m}^{-2}$
$\text{Chl} = 0.241 \times \text{MTCI} - 0.618$	0.90	0.38
$\text{Chl} = 18.509 \times \text{red edge NDVI}_{740} - 0.999$	0.91	0.37
$\text{Chl} = 6.645 \times \text{CI}_{740} - 0.649$	0.91	0.36

#### 4. Discussion

Three important factors affecting crop reflectance are (i) soil/residue background; (ii) foliar Chl and (iii) leaf area index/canopy density. In the present study, during the vegetative stage, foliar Chl increased slightly, especially in maize, although vegetation fraction and green LAI increased steadily from zero to maximal values. The tradeoff between the effect of decreasing soil/residue background and increasing vegetation fraction during crop development greatly influenced canopy reflectance in the vegetative stage.

Specifically, visible reflectance was high due to a significant contribution of high reflectance soil/residue at the beginning of the season in the vegetative stage. As the crop developed, vegetation cover and green LAI increased, masking the influence of the soil/residue background and decreasing visible and red edge reflectance. With increases in the green vegetation fraction above about 60% and canopy Chl above  $2.5 \text{ g}\cdot\text{m}^{-2}$  in maize and  $1.5 \text{ g}\cdot\text{m}^{-2}$  in soybean, canopy transmittance decreased due to high foliar Chl and LAI. Additionally, self-shadowing became significant, decreasing reflectance. The depth of light penetration inside the canopy (inversely proportional to leaf absorption and LAI) decreased and became limited by the upper leaf layers [33,62]. As a result, the slope of the reflectance vs. canopy Chl relationship decreased, and the sensitivity of canopy reflectance to canopy Chl dropped drastically, especially in the PAR regions (Figure 1A–D).

In the reproductive stage, green LAI decreased in accord with a decrease of foliar Chl; nevertheless, total LAI remained substantially high, masking the soil/residue background and reducing its effect on canopy reflectance during this stage. However, when canopy Chl was above  $2 \text{ g}\cdot\text{m}^{-2}$ , the decline of canopy Chl minimally affected absorbed radiation, and canopy reflectance was virtually invariant in the PAR and shortwave red edge regions [61]. This was due to the low transmittance of the canopy and the shortened path length of light inside the canopy [61,63]. When canopy Chl dropped below  $1.5 \text{ g}\cdot\text{m}^{-2}$ , the difference in reflectance between the two stages became increasingly significant, for the whole PAR range in maize (Figure 1A–C) and the blue and red regions in soybean (Figure 2A,C). At this period of senescence, leaf transmittance increased substantially, and the optical depth of the canopy in the PAR region increased. The amount of “illuminated chlorophyll” related to absorbed PAR became higher, and the whole canopy worked efficiently to absorb incident light [64]. Because of increasing chlorophyll efficiency [63], absorbed radiation was still substantial.

Thus, for the same canopy Chl, reflectance during senescence was lower than in the vegetative stage. These effects were especially pronounced in the blue and red regions with high chlorophyll absorption coefficients and less pronounced in the green and red edge regions where the absorption coefficients of chlorophyll are smaller [65].

In soybean, hysteresis in the green and red edge regions was absent. Reflectances in the early vegetative stage and the late senescence stage were almost the same (Figure 2B,D and Figure 3). This was because the soybean canopy architecture and leaf structure are very different from maize [47,63]. The soybean canopy was shorter (approximately 1 m vs. 3 m for maize) and appeared more “closed” to light penetration compared to maize due to the higher leaf area density (i.e., leaf area per unit canopy volume) in soybean. Maize was taller, and the canopy was much more “open” with a heterogeneous foliar Chl distribution where maximal Chl values were in the middle of the canopy [24]. This structural arrangement in maize was more favorable for deeper light penetration into the canopy than for soybean. In the reproductive stage, with decreases in canopy Chl, the maize canopy was capable of maintaining its high absorption capacity in the visible and red edge portions of the spectrum making reflectance lower than that in the vegetative stage. In soybean, with a decrease of foliar Chl during the reproductive stage, the penetration depth of light inside the leaves increased. Light reached the abaxial cell layers, which have a lower Chl than the adaxial layers and a decrease in absorption. Thus, reflectance increased to values similar to the early vegetative stage. Additionally, during senescence, light absorption by soybean decreased due to leaf inclination changes (e.g., folding leaves). This decreased the leaf surface area absorbing light. All of these factors contributed to increased reflectance for soybean in the reproductive stage.

Thus, different patterns of light absorption by crops with the same canopy Chl and different contributions of soil/residue to canopy reflectance in the vegetative and reproductive/senescence stages were the main reasons for the hysteresis, especially pronounced in the blue and red regions and less pronounced in the green and red edge regions. The hysteresis of reflectance and the differing structural properties of the crops studied brought uncertainties to canopy Chl estimation by VIs. Such hysteresis has the potential to influence other methods for estimating canopy Chl, such as machine learning and RTM. Some of these issues may be avoided by incorporating a temporal component into the analyses, but this is not in keeping with our goal of developing a generic model that can be applied for both crops without a priori knowledge of the crop phenological stage.

The accuracy of canopy Chl estimation by VIs using red edge and NIR bands was much higher than VIs with NIR and either red and green bands. This was due to the reduced sensitivity of the red edge to hysteresis driven by different canopy architectures and leaf structures. These features allowed the development of generic algorithms for the two different crops that successfully estimated canopy Chl throughout the entire growing season using spectral bands of the MSI sensor on board the Sentinel-2 satellite.

## 5. Conclusions

Crop phenology was a strong factor influencing canopy reflectance in two contrasting crops, maize and soybean. Phenology caused a substantial species-specific difference in the reflectance vs. canopy Chl relationships between the vegetative and reproductive stages. The reasons for the hysteresis were seasonal changes in canopy architecture, leaf structure and foliar Chl, as well as seasonal changes in the influence of the soil/residue background. The effect of the hysteresis on vegetation indices applied for canopy Chl estimation depended on the bands selected in their formulation. For widely-used VIs using NIR and red reflectance, NDVI, SR and EVI, there were significant differences in the VI vs. canopy Chl relationships between the vegetative and reproductive stages and between species, limiting their application for accurate canopy Chl estimation over the entire growing season. VIs with red edge and NIR bands, using reflectance simulated for the MSI sensor aboard Sentinel-2, included the  $CI_{740}$ , MTCI and red edge  $NDVI_{740}$ . These VIs were accurate in estimating canopy Chl in maize and soybean with RMSE values below  $0.38 \text{ g}\cdot\text{m}^{-2}$ . Algorithms utilizing these VIs did not require separate parameterization for each crop nor each phenological stage.

Despite encouraging results, thoughtful studies of reflectance vs. canopy Chl relationships are still required for different types of crops with contrasting biochemical and structural properties. The robustness of generic algorithms for different crops and their varieties should be confirmed in further studies. These algorithms should also be examined for their sensitivity to a range of typical soil backgrounds.

**Acknowledgments:** We sincerely appreciate the support and use of the facilities and data provided by the Center for Advanced Land Management Information Technologies (CALMIT) and the Carbon Sequestration Program at the University of Nebraska-Lincoln. Y.P. was supported by the National 863 Project of China (2013AA102401), and the National Natural Science Foundation of China (41401390). A.G. was supported by the Marie Curie International Incoming Fellowship at Technion, Israel. The US-Ne1, US-Ne2 and US-Ne3 AmeriFlux sites are supported by the Lawrence Berkeley National Lab AmeriFlux Data Management Program and by the Carbon Sequestration Program, University of Nebraska-Lincoln Agricultural Research Division. Funding for AmeriFlux core site data was provided by the U.S. Department of Energy's Office of Science.

**Author Contributions:** Yi Peng and Anatoly Gitelson conceived the project. Timothy Arkebauer and Anatoly Gitelson collected or provided in situ reflectance and LAI data. Yi Peng, Anatoly Gitelson and Anthony Nguy-Robertson performed data analysis. Yi Peng and Anatoly Gitelson drafted the manuscript. All authors contributed to discussion and preparation of the manuscript.

**Conflicts of Interest:** The authors declare no conflict of interest.

**Abbreviations**

The following abbreviations were used in text:

- Chl Chlorophyll content
- MSI Multi Spectral Instrument
- VI Vegetation index
- RTM Radiative transfer model
- LAI Leaf area index
- NIR Near-infrared
- NDVI Normalized difference vegetation index
- SR Simple ratio
- EVI Enhanced vegetation index
- CI Chlorophyll index
- MTCI MERIS terrestrial chlorophyll index
- R<sup>2</sup> Determination coefficient
- RMSE Root mean square error
- NRMSE Normalized root mean square error
- PAR Photosynthetically-active radiation

**Appendix A**

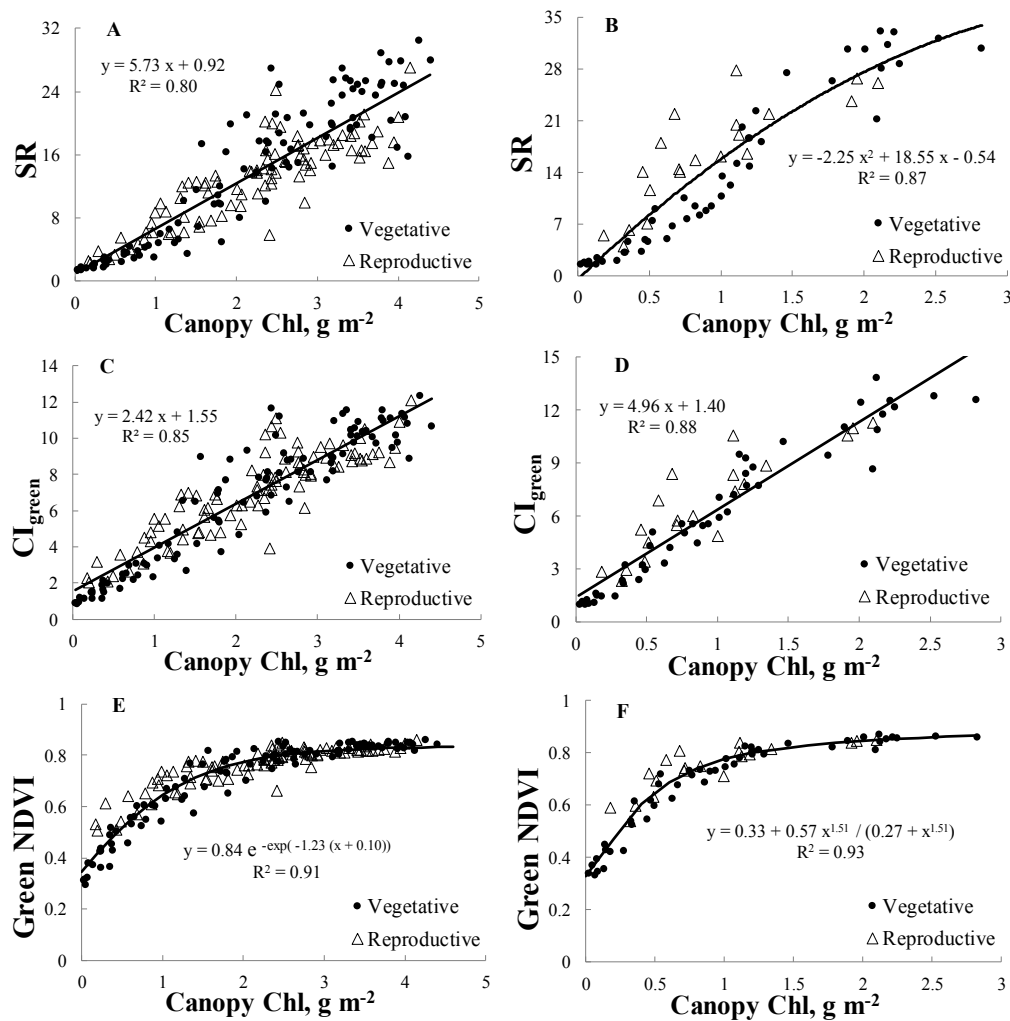
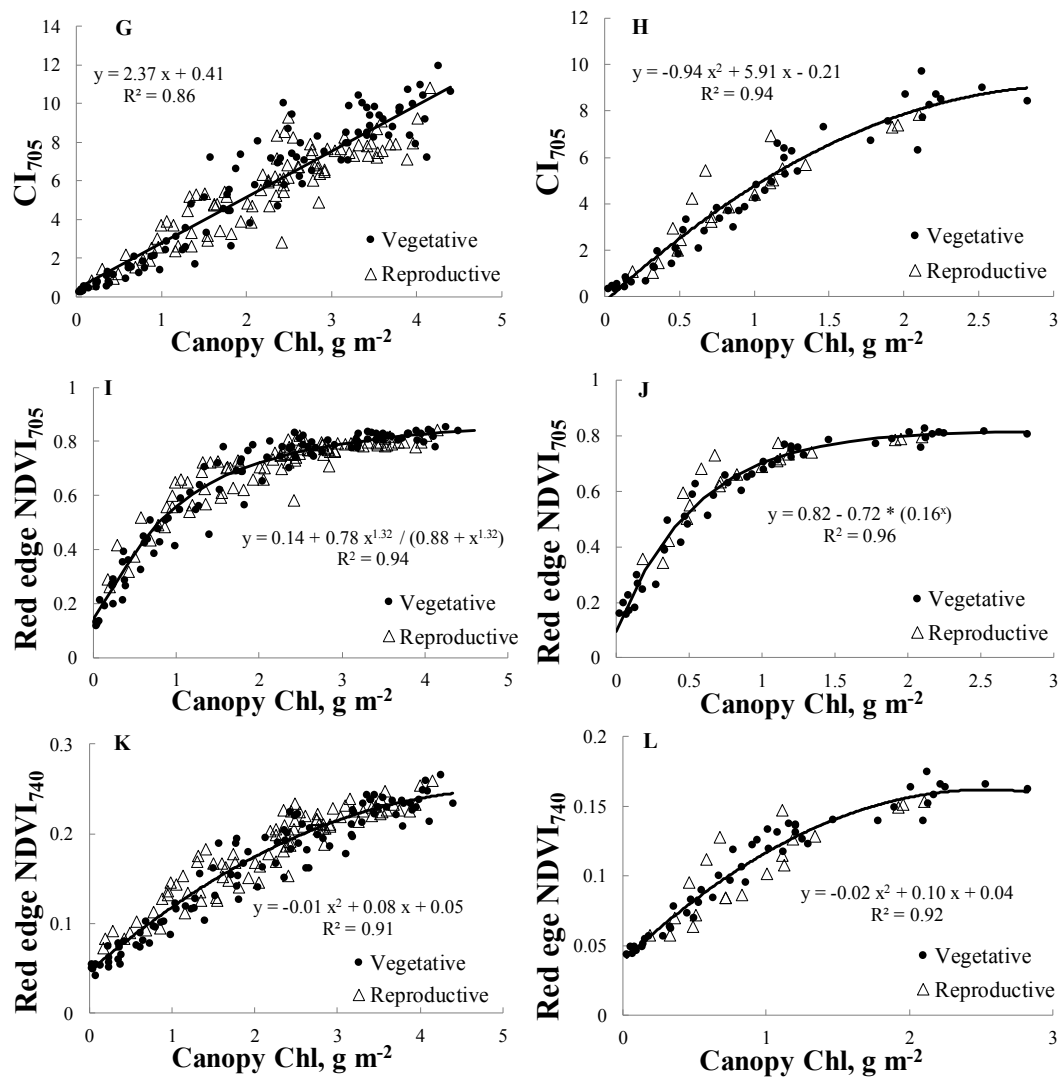


Figure A1. Cont.



**Figure A1.** Relationships of VI vs. canopy Chl during both growth stages for SR in maize (A), SR in soybean (B),  $CI_{green}$  in maize (C),  $CI_{green}$  in soybean (D), green NDVI in maize (E), green NDVI in soybean (F),  $CI_{705}$  in maize (G),  $CI_{705}$  in soybean (H), red edge  $NDVI_{705}$  in maize (I), red edge  $NDVI_{705}$  in soybean (J), red edge  $NDVI_{740}$  in maize (K) and red edge  $NDVI_{740}$  in soybean (L). The solid line represents the best-fit-function of VI vs. canopy Chl developed using samples from the vegetative and reproductive stages combined.

## References

- Osborne, B.A.; Raven, J.A. Light absorption by plants and its implications for photosynthesis. *Biol. Rev. Camb. Philos. Soc.* **1986**, *61*, 1–60. [[CrossRef](#)]
- Curran, P.J.; Dungan, J.L.; Gholz, H.L. Exploring the relationship between reflectance red edge and chlorophyll content in slash pine. *Tree Physiol.* **1990**, *7*, 33–48. [[CrossRef](#)] [[PubMed](#)]
- Farquhar, G.D.; Sharkey, T.D. Stomatal conductance and photosynthesis. *Ann. Rev. Plant Physiol.* **1982**, *33*, 317–345. [[CrossRef](#)]
- Sharkey, T.D. Photosynthesis in intact leaves of C3 plants: Physics, physiology and rate limitations. *Bot. Rev.* **1985**, *51*, 53–105. [[CrossRef](#)]
- Houborg, R.; McCabe, M.; Cescatti, A.; Gao, F.; Schull, M.; Gitelson, A. Joint leaf chlorophyll content and leaf area index retrieval from Landsat data using a regularized model inversion system (REGFLEC). *Remote Sens. Environ.* **2015**, *159*, 203–221. [[CrossRef](#)]

6. Evans, J.R. Photosynthesis and nitrogen relationships in leaves of C3 plants. *Oecologia* **1989**, *78*, 9–19. [[CrossRef](#)]
7. Baret, F.; Houles, V.; Guerif, M. Quantification of plant stress using remote sensing observations and crop models: The case of nitrogen management. *J. Exp. Bot.* **2007**, *58*, 869–880. [[CrossRef](#)] [[PubMed](#)]
8. Filella, I.; Serrano, L.; Serra, J.; Penuelas, J. Evaluating wheat nitrogen status with canopy reflectance indices and discriminant analysis. *Crop. Sci.* **1995**, *35*, 1400–1405. [[CrossRef](#)]
9. Sage, R.F.; Percy, R.W.; Seemann, J.R. The nitrogen use efficiency of C3 and C4 plants. *Plant Physiol.* **1987**, *85*, 355–359. [[CrossRef](#)] [[PubMed](#)]
10. Schlemmer, M.; Gitelson, A.; Schepers, J.; Ferguson, R.; Peng, Y.; Shanahan, J.; Rundquist, D. Remote estimation of nitrogen and chlorophyll contents in maize at leaf and canopy levels. *Int. J. Appl. Earth. Obs.* **2013**, *25*, 47–54. [[CrossRef](#)]
11. Evans, J.R. Photosynthesis in the Flag Leaf of Wheat (*Triticum aestivum* L.). *Plant Physiol.* **1983**, *72*, 297–302. [[CrossRef](#)] [[PubMed](#)]
12. Gitelson, A.A.; Viña, A.; Ciganda, V.; Rundquist, D.C.; Arkebauer, T.J. Remote estimation of canopy chlorophyll content in crops. *Geophys. Res. Lett.* **2005**, *32*, 93–114. [[CrossRef](#)]
13. Gitelson, A.A.; Viña, A.; Verma, S.B.; Rundquist, D.C.; Arkebauer, T.J.; Keydan, G.; Leavitt, B.; Ciganda, V.; Burba, G.G.; Suyker, A.E. Relationship between gross primary production and chlorophyll content in crops: Implications for the synoptic monitoring of vegetation productivity. *Geophys. Res. Lett.* **2006**, *111*, 854–871. [[CrossRef](#)]
14. Harris, A.; Dash, J. The potential of the MERIS Terrestrial chlorophyll Index for carbon flux estimation. *Remote Sens. Environ.* **2010**, *114*, 1856–1862. [[CrossRef](#)]
15. Wu, C.; Wang, L.; Niu, Z.; Gao, S.; Wu, M.Q. Nondestructive estimation of canopy chlorophyll content using Hyperion and Landsat/TM images. *Int. J. Remote Sens.* **2010**, *31*, 2159–2167. [[CrossRef](#)]
16. Peng, Y.; Gitelson, A.A.; Keydan, G.P.; Rundquist, D.C.; Moses, W.J. Remote estimation of gross primary production in maize and support for a new paradigm based on total crop chlorophyll content. *Remote Sens. Environ.* **2011**, *115*, 978–989. [[CrossRef](#)]
17. Clevers, J.G.P.W.; Kooistra, L. Using hyperspectral remote sensing data for retrieving canopy chlorophyll and nitrogen content. *IEEE J. Sel. Top. Appl. Earth Obs. Remote Sens.* **2012**, *5*, 574–583. [[CrossRef](#)]
18. Féret, J.B.; François, C.; Gitelson, A.; Asner, G.P.; Barry, K.M.; Panigada, C.; Richardson, A.; Jacquemoud, S. Optimizing spectral indices and chemometric analysis of leaf chemical properties using radiative transfer modeling. *Remote Sens. Environ.* **2011**, *115*, 2742–2750. [[CrossRef](#)]
19. Féret, J.-B.; Gitelson, A.A.; Noble, S.D.; Jacquemoud, S. PROSPECT-D: Towards modeling leaf optical properties through a complete lifecycle. *Remote Sens. Environ.* **2017**. accepted.
20. Ustin, S.L.; Gitelson, A.A.; Jacquemoud, S.; Schaepman, M.; Asner, G.P.; Gamon, J.A.; Zarco-Tejada, P. Retrieval of foliar information about plant pigment systems from high resolution spectroscopy. *Remote Sens. Environ.* **2009**, *113*, S67–S77. [[CrossRef](#)]
21. Bacour, C.; Baret, F.; Béal, D.; Weiss, M.; Pavageau, K. Neural network estimation of LAI, fAPAR, fCover and LAIxCab, from top of canopy MERIS reflectance data: Principles and validation. *Remote Sens. Environ.* **2006**, *105*, 313–325. [[CrossRef](#)]
22. Gitelson, A.A.; Gritz, U.; Merzlyak, M.N. Relationships between leaf chlorophyll content and spectral reflectance and algorithms for non-destructive chlorophyll assessment in higher plant leaves. *J. Plant Physiol.* **2003**, *160*, 271–282. [[CrossRef](#)] [[PubMed](#)]
23. Dash, J.; Curran, P.J. The MERIS terrestrial chlorophyll index. *Int. J. Remote Sens.* **2004**, *25*, 5003–5013. [[CrossRef](#)]
24. Ciganda, V.; Gitelson, A.A.; Schepers, J. Vertical profile and temporal variation of chlorophyll in maize canopy: Quantitative “Crop Vigor” indicator by means of reflectance-based techniques. *Agron. J.* **2008**, *100*, 1409–1417. [[CrossRef](#)]
25. Weiss, M.; Baret, F.; Smith, G.J.; Jonckheere, I.; Coppin, P. Review of methods for in situ leaf area determination. Part II. Estimation of LAI, errors and sampling. *Agric. For. Meteorol.* **2004**, *121*, 37–53. [[CrossRef](#)]
26. Gausman, H.W.; Allen, W.A.; Cardenas, R.; Richardson, A.J. Effects of leaf nodal position on absorption and scattering coefficients and infinite reflectance of cotton leaves, *Gossypium hirsutum* L. *Agron. J.* **1971**, *63*, 87–91. [[CrossRef](#)]

27. Gausman, H.W.; Rodriguez, R.R.; Richardson, A.J. Infinite reflectance of dead compared with live vegetation. *Agron. J.* **1976**, *68*, 295–296. [[CrossRef](#)]
28. Asrar, G.; Fuchs, M.; Kanemasu, E.T.; Hatfield, J.L. Estimation absorbed photosynthetic radiation and leaf area index from spectral reflectance in wheat. *Agron. J.* **1984**, *76*, 300–306. [[CrossRef](#)]
29. Asrar, G.; Kanemasu, E.T.; Yoshida, M. Estimates of leaf area index from spectral reflectance of wheat under different cultural practices and solar angle. *Remote Sens. Environ.* **1985**, *17*, 1–11. [[CrossRef](#)]
30. Hatfield, J.L.; Asrar, G.; Kanemasu, E.T. Intercepted photosynthetically active radiation estimated by spectral reflectance. *Remote Sens. Environ.* **1984**, *14*, 65–75. [[CrossRef](#)]
31. Wiegand, C.L.; Gerbermann, A.H.; Gallo, K.P.; Blad, B.L.; Dusek, D. Multisite analyses of spectral-biophysical data for corn. *Remote Sens. Environ.* **1990**, *33*, 1–16. [[CrossRef](#)]
32. Potitthep, S.; Nagai, S.; Nasahara, K.N.; Muraoka, H.; Suzuki, R. Two separate periods of the LAI–VI relationships using in situ measurements in a deciduous broadleaf forest. *Photosynth. Res.* **2013**, *169*, 148–155. [[CrossRef](#)]
33. Sellers, P.J. Canopy reflectance, photosynthesis, and transpiration. *Int. J. Remote Sens.* **1985**, *8*, 1335–1372. [[CrossRef](#)]
34. Delegido, J.; Verrelst, J.; Rivera, G.P.; Ruiz-Verdú, A.; Moreno, J. Brown and green LAI mapping through spectral indices. *Int. J. Appl. Earth. Obs.* **2015**, *35*, 350–358. [[CrossRef](#)]
35. Kokaly, R.F.; Asner, G.P.; Ollinger, S.V.; Martin, M.E.; Wessman, C.A. Characterizing canopy biochemistry from imaging spectrometer data for studying ecosystem processes. *Remote Sens. Environ.* **2009**, *113*, S78–S91. [[CrossRef](#)]
36. Delegido, J.; Verrelst, J.; Alonso, L.; Moreno, J. Evaluation of Sentinel-2 red-edge bands for empirical estimation of green LAI and chlorophyll content. *Sensors* **2011**, *11*, 7063–7081. [[CrossRef](#)] [[PubMed](#)]
37. Delegido, J.; Verrelst, J.; Meza, C.M.; Rivera, J.P.; Alonso, L.; Moreno, J. A red-edge spectral index for remote sensing estimation of green LAI over agroecosystems. *Eur. J. Agron.* **2013**, *46*, 42–52. [[CrossRef](#)]
38. Di Bella, C.M.; Paruelo, M.J.; Becerra, J.E.; Bacour, C.; Baret, F. The effect of senescent leaves on the estimation of the fraction of photosynthetically active radiation absorbed by the green elements of the canopy (fAPAR<sub>g</sub>) from NDVI measurements. *Int. J. Remote Sens.* **2004**, *25*, 5415–5427. [[CrossRef](#)]
39. Van Leeuwen, W.J.D.; Huete, A.R. Effects of standing litter on the biophysical interpretation of plant canopies with spectral indices. *Remote Sens. Environ.* **1996**, *55*, 123–138. [[CrossRef](#)]
40. Asner, G.P. Biophysical and biochemical sources of variability in canopy reflectance. *Remote Sens. Environ.* **1998**, *64*, 234–253. [[CrossRef](#)]
41. Sellers, P.J. Vegetation-canopy spectral reflectance and biophysical processes. In *Theory and Applications of Optical Remote Sensing*; Asrar, G., Ed.; John Wiley and Sons: New York, NY, USA, 1989; pp. 297–333.
42. Viña, A.; Henebry, G.M.; Gitelson, A.A. Satellite monitoring of vegetation dynamics: Sensitivity enhancement by the Wide Dynamic Range Vegetation Index. *Geophys. Res. Lett.* **2004**, *31*, 373–394. [[CrossRef](#)]
43. Drusch, M.; Del Bello, U.; Carlier, S.; Colin, O.; Fernandez, V.; Gascon, F.; Hoersch, B.; Isola, C.; Laberinti, P.; Martimort, P.; et al. Sentinel-2: ESA's optical high-resolution mission for GMES operational services. *Remote Sens. Environ.* **2012**, *120*, 25–36. [[CrossRef](#)]
44. Verma, S.B.; Dobermann, A.; Cassman, K.G.; Walters, D.T.; Knops, J.M.; Arkebauer, T.J.; Suyker, A.E.; Burba, G.G.; Amos, B.; Yang, H.; et al. Annual carbon dioxide exchange in irrigated and rainfed maize-based agroecosystems. *Agric. For. Meteorol.* **2005**, *131*, 77–96. [[CrossRef](#)]
45. Rundquist, D.C.; Perk, R.; Leavitt, B.; Keydan, G.P.; Gitelson, A.A. Collecting spectral data over cropland vegetation using machine-positioning versus hand-positioning of the sensor. *Comput. Electron. Agric.* **2004**, *43*, 173–178. [[CrossRef](#)]
46. Rundquist, D.C.; Gitelson, A.A.; Leavitt, B.; Zyguelbaum, A.; Perk, R.; Keydan, G.P. Elements of an integrated phenotyping system for monitoring crop status at canopy level. *Agronomy* **2014**, *4*, 108–123. [[CrossRef](#)]
47. Viña, A.; Gitelson, A.; Nguy-Robertson, A.L.; Peng, Y. Comparison of different vegetation indices for the remote assessment of green leaf area index of crops. *Remote Sens. Environ.* **2011**, *115*, 3468–3478. [[CrossRef](#)]
48. Ciganda, V.; Gitelson, A.A.; Schepers, J. Non-destructive determination of maize leaf and canopy chlorophyll content. *J. Plant Physiol.* **2009**, *166*, 157–167. [[CrossRef](#)] [[PubMed](#)]
49. Ritchie, S.W.; Hanway, J.J.; Thompson, H.E.; Benson, G.O. *How A Soybean Plant Develops*; Special Report No. 53; Iowa State University: Ames, IA, USA, 1985; p. 24.

50. Atzberger, C.; Richter, K. Spatially constrained inversion of radiative transfer models for improved LAI mapping from future Sentinel-2 imagery. *Remote Sens. Environ.* **2012**, *120*, 208–218. [[CrossRef](#)]
51. Verrelst, J.; Camps-Valls, G.; Muñoz-Mari, J.; Rivera, J.P.; Veroustraete, F.; Clevers, G.P.W.; Moreno, J. Optical remote sensing and the retrieval of terrestrial vegetation bio-geophysical properties—A review. *ISPRS J. Photogramm. Remote Sens.* **2015**, *108*, 273–290. [[CrossRef](#)]
52. Vincini, M.; Calegari, F.; Casa, R. Sensitivity of leaf chlorophyll empirical estimators obtained at Sentinel-2 spectral resolution for different canopy structures. *Precis. Agric.* **2016**, *17*, 313–331. [[CrossRef](#)]
53. Clevers, J.G.P.W.; Gitelson, A.A. Remote estimation of crop and grass chlorophyll and nitrogen content using red-edge bands on Sentinel-2 and -3. *Int. J. Appl. Earth. Obs.* **2013**, *23*, 344–351. [[CrossRef](#)]
54. Jordan, C.F. Derivation of leaf area index from quality of light in the forest floor. *Ecology* **1969**, *50*, 663–666. [[CrossRef](#)]
55. Rouse, J.W.; Haas, R.H., Jr.; Schell, J.A.; Deering, D.W. Monitoring vegetation systems in the Great Plains with ERTS. In *NASA SP-351 Third ERTS-1 Symposium*; Fraden, S.C., Marcanti, E.P., Becker, M.A., Eds.; Scientific and Technical Information Office, National Aeronautics and Space Administration: Washington, DC, USA, 1974; pp. 309–317.
56. Huete, A.R.; Liu, H.Q.; Batchily, K.; van Leeuwen, W. A comparison of vegetation indices global set of TM images for EOS-MODIS. *Remote Sens. Environ.* **1997**, *59*, 440–451. [[CrossRef](#)]
57. Viña, A.; Gitelson, A.A. New developments in the remote estimation of the fraction of absorbed photosynthetically active radiation in crops. *Geophys. Res. Lett.* **2005**, *32*, 195–221.
58. Fielding, A.L.; Bell, J.F. A review of methods for the assessment of prediction errors in conservation presence/absence models. *Environ. Conserv.* **1997**, *24*, 38–49. [[CrossRef](#)]
59. Kohavi, R. A study of cross-validation and bootstrap for accuracy estimation and model selection. In *Proceedings of the 14th International Joint Conference on Artificial Intelligence*, Montreal, QC, Canada, 20–25 August 1995; pp. 1137–1145.
60. Snedecor, G.W.; Cochran, W.G. *Statistical Methods*, 8th ed.; Iowa State University Press: Ames, IA, USA, 1989.
61. Gitelson, A.A.; Peng, Y.; Arkebauer, T.J.; Schepers, J. Relationships between gross primary production, green LAI, and canopy chlorophyll content in maize: Implications for remote sensing of primary production. *Remote Sens. Environ.* **2014**, *144*, 65–72. [[CrossRef](#)]
62. Merzlyak, M.; Gitelson, A.A. Why and what for the leaves are yellow in autumn? On the interpretation of optical spectra of senescing leaves (*Acer platanoides* L.). *J. Plant Physiol.* **1995**, *145*, 315–320. [[CrossRef](#)]
63. Gitelson, A.A.; Peng, Y.; Vina, A.; Arkebauer, T.; Schepers, J.S. Efficiency of chlorophyll in gross primary productivity: A proof of concept and application in crops. *J. Plant Physiol.* **2016**, *201*, 101–110. [[CrossRef](#)] [[PubMed](#)]
64. Gamon, J.A. Optical sampling of the flux tower footprint. *Biogeosciences* **2015**, *12*, 4509–4523. [[CrossRef](#)]
65. Lichtenthaler, H.K. Chlorophyll and carotenoids: Pigments of photosynthetic biomembranes. *Methods Enzymol.* **1987**, *148*, 331–382.

